

We are IntechOpen, the world's leading publisher of Open Access books Built by scientists, for scientists

6,900

Open access books available

186,000

International authors and editors

200M

Downloads

Our authors are among the

154

Countries delivered to

TOP 1%

most cited scientists

12.2%

Contributors from top 500 universities



WEB OF SCIENCE™

Selection of our books indexed in the Book Citation Index
in Web of Science™ Core Collection (BKCI)

Interested in publishing with us?
Contact book.department@intechopen.com

Numbers displayed above are based on latest data collected.
For more information visit www.intechopen.com



Ceramic Preparation of Nanopowders and Experimental Investigation of Its Properties

Sergey Bardakhanov, Vladimir Lysenko,
Andrey Nomoev¹ and Dmitriy Trufanov

*Khristianovich Institute of Theoretical and Applied Mechanics of
Siberian Branch of Russian Academy of Science, Novosibirsk,*

*¹Buryatian State University, Ulan Ude,
Russia*

1. Introduction

Particles of the sizes less than 100 nm (nanoparticles) provide new properties to the materials. For example, the quantum confinement of carriers within small nanocrystals enables the tuning of optical properties with a particle size that led to the demonstration of nanostructured light emitting diodes (Colvin et al., 1994). Metal nanopowders obtained in an electron accelerator (Lukashov et al., 1996), (Bardakhanov et al., 2008) through the evaporation of initial materials exhibit high catalytic properties (Korchagin et al., 2005) and silicon nanopowders exposed to ultraviolet radiation reemit in the visible blue-green spectral range (Efremov et al., 2004).

The design and preparation of nanoceramics from nanopowders is one of the directions of modern nanotechnology. Special effort has been directed toward retaining the smallest possible grains in the final product. It is known that the development of dislocations is terminated at the grain boundaries. Hence, it follows that the smaller the size of grains in the ceramics and the more developed the grained structure, the higher strength of the ceramic material. It is assumed that nanoceramics will have some other unique characteristics (for example, superplasticity (Zhou Xinzhang et al., 2005)). The preparation of fine-grained ceramics with a homogenous structure has opened up new possibilities for wide application of these materials in many fields, for example, in structural elements of engines, cutting tools, bioceramics (as coatings for implants), corrosion-resistant and wear-resistant coatings, insulators with high dielectric properties, and so on.

The purpose of the present work was to prepare dense high-strength ceramics with a small grain size (of the order of several microns) from nanopowders.

2. Experimental procedure

The nanopowders of different manufacturers were used as raw material, including the ones obtained by evaporation at the electron beam accelerator with the subsequent condensation of substance as nanosize particles (Lukashov et al., 1996), (Bardakhanov et al., 2008). Ceramic compositions were both pure, and constituted of several components. The nanosize powders of the following chemical components were used: silica SiO_2 , alumina Al_2O_3 ,

titania TiO_2 , aluminium nitride AlN , tungsten carbide WC , gadolinium oxide Gd_2O_3 and yttrium oxide Y_2O_3 .

In our experiments we reproduced the main stages of the ceramic production: (i) the preparation of the initial materials in the form of nanopowders, (ii) their granulation, (iii) molding of raw pellets from powder materials, (iv) heat treatment, and (v) analysis of the ceramic samples. In the main stage of the compression molding, we used steel molds 25 mm in diameter. The preliminary heat treatment of nanopowders and their sintering were performed in furnaces with air atmosphere (for all oxides), nitrogen atmosphere (for AlN) and in vacuum (for WC).

The properties of the ceramic samples thus prepared were investigated using scanning electron microscopy (JSM-6460 LV (Jeol) electron microscope, Japan), transmission electron microscopy (JEM-100CX, Japan) and X-ray powder diffraction (HZG-4 diffractometer, monochromatic Co radiation). The specific surface area was determined with the use of an Quantachrome Autosorb-6B-Kr automated adsorption analyzer (United States) with nitrogen as an adsorbing agent. The optical properties were evaluated on an SF-56 spectrophotometer. The microhardness was determined using PMT-3 device. Ultimate compression strength was determined using the machine for material strength test Zwick/Roell Z005 (Germany).

3. Results and discussion

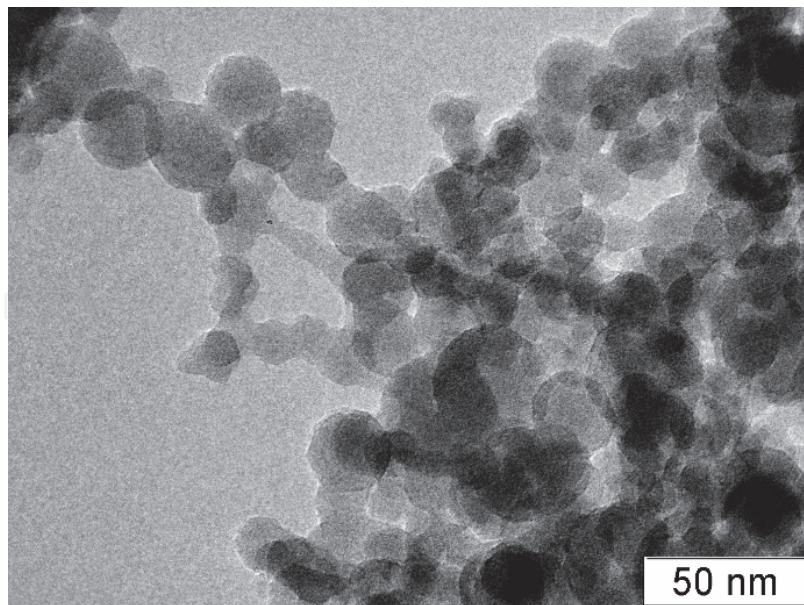
3.1 Silicon dioxide SiO_2

The nanopowders of two groups were used: (1) tarkosil (Lukashov et al., 1996), (Bardakhanov et al., 2008) with the specific surface of 50-220 m^2/g and the average size of particles 13-60 nm, (2) aerosil hydrophilic powders (Degussa, Germany) with the specific surface of 90 and 380 m^2/g . All the powders under investigation were X-ray amorphous without impurities of a crystalline phase (reflections in the X-ray diffraction patterns are absent).

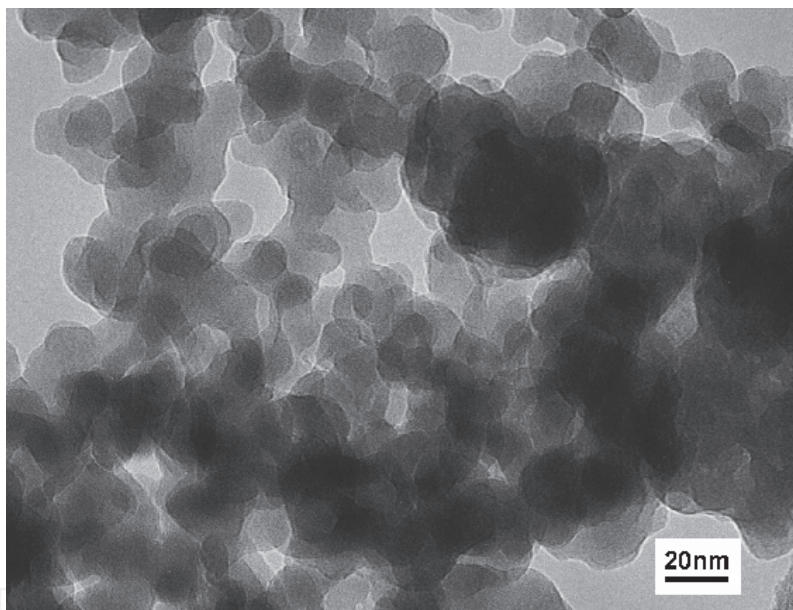
At the maximum temperature $T_{\text{max}}=1000^\circ\text{--}1620^\circ\text{C}$ the sintered tarkosil samples had greater strength, than aerosil samples, but less shrinkage. It seems, it is due to distinctions in ways of tarkosil and aerosil production. One can assume also, that greater aerosil samples shrinkage (sometimes it was about 40%, and for tarkosil it usually was 20-25%) is caused by different shape of agglomerates, although TEM images of tarkosil and aerosil have shown that they are similar (see Fig. 1(a,b)).

The tarkosil powders of SiO_2 initially were subjected to dry pressing and then were sintered. Dry pressing directly resulted in the formation of relatively high-strength pellets only with the use of step-by-step loading. However, with excess of a particular thickness of the raw pellet, it underwent separation into layers. Apparently, the reason for this separation is the existence of elastic agglomerates in the initial powders.

Nonetheless, the pressed samples of tarkosil were subjected to heat treatment, during which they began to be sintered already at the temperature of 1000°C without a change in the white or grayish (depending on the powder type) color of the surface and fracture. The heat-treated samples were not destroyed during moistening. The examination of these samples with a scanning electron microscope revealed the formation of aggregates of sintered particles. The samples obtained at the temperature of 1500°C exhibited indications of the onset of the vitrification on the surface. The heat treatment at the temperature $T_{\text{max}} = 1620^\circ\text{C}$ in all cases resulted in the formation of ceramic materials that either were separated along the layers into fragments, or were substantially deformed.



(a)



(b)

Fig. 1. TEM image of SiO₂ nanopowders: tarkosil T-25 (obtained with using electron accelerator) (a), aerosil A-380 (Degussa, Germany) (b).

At the next stage, the tarkosil powders were subjected to dispersion in distilled water until the formation of a creamy substance, which was dried for several days at room temperature. The grains obtained after drying were passed through sieves. The fraction with sizes larger than 1 mm and smaller than 2 mm was subjected to step-by-step pressing. This procedure resulted in the formation of non-layered raw pellets with a strength high enough to transfer them to the furnace. These pellets were sequentially sintered under specified temperature-time conditions with isothermal exposure at the temperature $T_{\max} = 1600^{\circ}\text{C}$. As a result, the samples retained their shape without separation into layers. Their ultimate compression

strength was 0.2 GPa about, and microhardness – 2 GPa about. Their surface was vitrified; however they had a different internal structure.

Fig. 2 displays the scanning electron microscope image of the cleavage of the sample sintered from 1- to 2-mm grains of the T-15 tarkosil nanopowder (primary particles size of 25 nm) after the preliminary heat treatment and isothermal exposure at the temperature of 1600°C for 5 h. It can be seen from this figure that the ceramics prepared has the fine-grained nonporous internal structure (with the grain size of the order of 10–20 μm). Although the process of grain transformation requires further investigation, the comparison with the data obtained from analyzing the scanning electron microscope image of the sample surface gives grounds to believe that a more prolonged isothermal exposure should result in the formation of the glassy state throughout the volume of the sample. In particular, the glassy state with a relatively high transparency has already been obtained in thin fragments of some samples after their pressing and sintering.

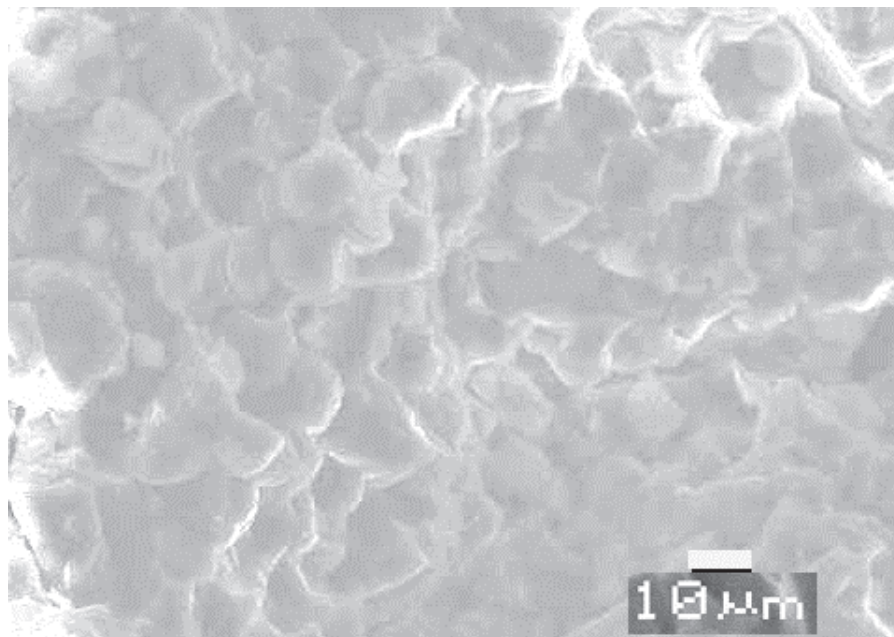


Fig. 2. SEM image of the sample sintered from 1-2 mm grains of the T-15 tarkosil (silicon dioxide) nanopowder with exposure at a temperature of 1660°C.

For one of the glassy samples (tarkosil T-20, sintered at 1620°C), we evaluated the optical properties. The transparency of this sample for waves with a length of more than 330 nm in the visible spectrum was below the corresponding value for a commercial window glass. However, for waves with a length of 270–330 nm (in the ultraviolet range), the transparency of the prepared glass was higher than that in the case of the window glass.

It can be expected that, apart from ceramics, tarkosils can serve as initial components for the preparation of silica glasses and quartz fibers. For the latter purpose, the T-05 tarkosil powder (specific surface area, 50 m²/g) with an extremely low content of OH groups on the surface and inside the particles can prove to be especially useful, although the method used for treatment of this powder, certainly, should differ from that described above. We note also that the use of different modifiers (see (Iler, 1979), for example), apparently, will make it possible to obtain a wide variety of glasses based on tarkosils

3.2 Aluminium oxide Al_2O_3

Powders of alumina were processed as pure, as in compositions. The powders AKP-50 (with average size of primary particles $d_{av} \sim 200$ nm) and AM-21 ($d_{av} \sim 4$ μm) (Sumitomo Chemicals, Japan), Aluminum Oxide C ($d_{av} = 13$ nm (Bode et al.), Degussa, Germany), plasma-chemical A ($d_{av} \sim 300$ nm, Siberian Chemical Plant) and B, obtained by the method^{2,3} ($d_{av} = 33$ nm) were used as basis. The powders of magnesia SG ($d_{av} = 73$ nm, Sukkyoung Co, Republic of Korea) and silica A-380 ($d_{av} = 7$ nm, Degussa) were used as modifiers.

Past experiments on dry pressing pure powders showed that the strength of pressed samples increases in the following course: A (300 nm), Aluminum Oxide C (13 nm), AM-21 (4 μm), B (33 nm), AKP-50 (200 nm). It seems that the strength of pressed samples is determined not by the size of primary particles, but by the kind of agglomerates, which are the consequence of method to obtain powders. One can assume, that compressibility (as well as the form of agglomerates) is determined by phase of substance, and it directly influences the bonding of particles.

The investigation of powders had shown that in plasma-chemical powder A the alumina phases δ - and θ - are present in about equal quantities. While Aluminum Oxide C and powder B entirely consist of the phase γ -, and AM-21 and AKP-50 almost entirely consist of the phase α -. It can be assumed that the structure and form of agglomerates and phase composition of powders affect the level of particles adhesion during loading, which ultimately determines the strength of pressed samples.

In accordance with the above sequence the microhardness and strength of sintered samples varied – the microhardness: A (0.4 GPa), Aluminum Oxide C (1.5 GPa), AM-21 (2.8 GPa), B (3.1 GPa), AKP-50 (9 GPa), the ultimate compression strength, beginning with AM-21, exceeds 0.3 GPa, and for the most strong ceramics from AKP-50 the strength was more 1 GPa.

The strength and microhardness of sample from the powder B (33 nm, obtained in an electron accelerator) was found to be rather unexpectedly high, because, on X-ray investigation data, this powder initially almost entirely consists of the phase γ - Al_2O_3 of boehmite row. Fig. 3 shows the particle size distribution for Al_2O_3 nanopowder obtained with using electron accelerator.

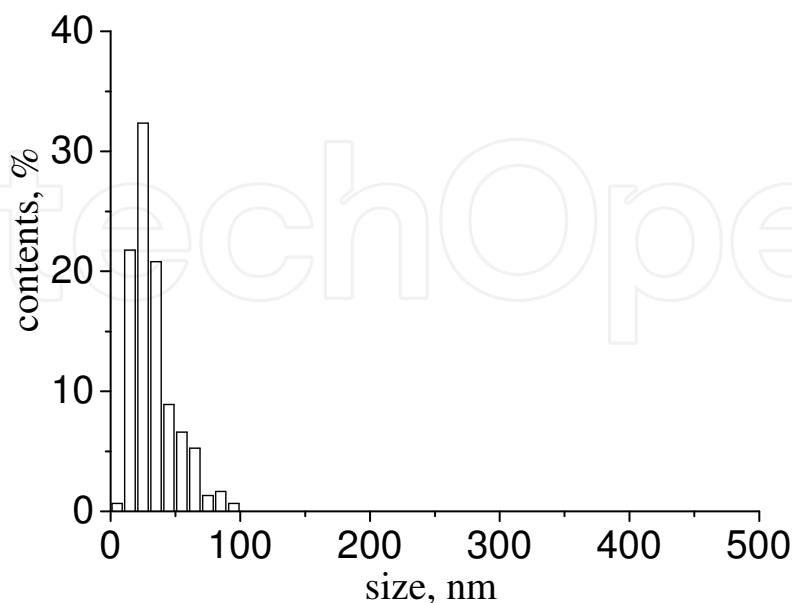
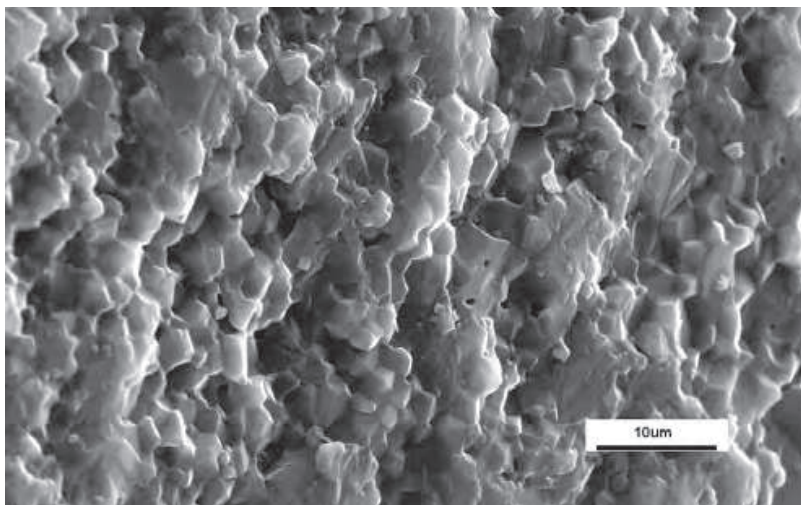


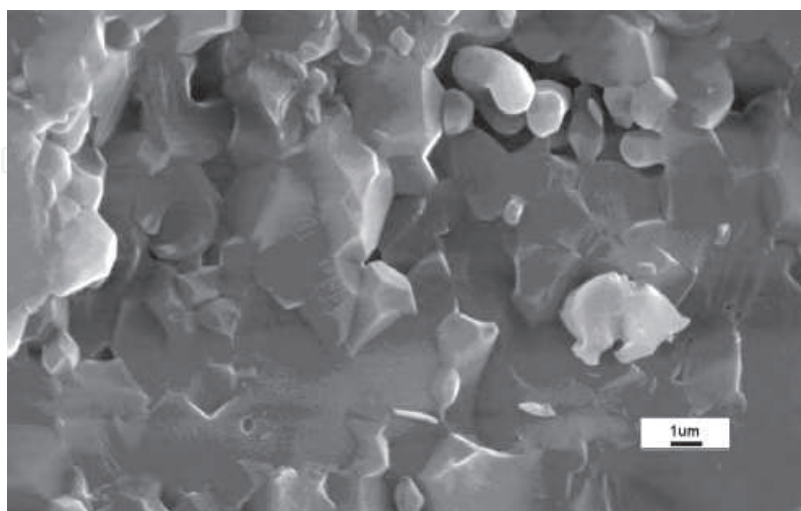
Fig. 3. Particle size distribution for Al_2O_3 nanopowder obtained with using electron accelerator.

The task of preparation of hard and dense electroceramics on the basis of alumina with additives was set. Different compositions were used. Sintering was done at $T_{\max}=1500^{\circ}\text{C}$. The greatest density, strength and microhardness was reached in samples of such composition: AKP-50 (Sumitomo Chemicals, Japan, the average size of primary particles $d\sim 200\text{ nm}$) - modifier SG (magnesia, $d=73\text{ nm}$, Sukkyoung Co, South Korea) - Aluminum Oxide C ($d=13\text{ nm}$, Degussa, Germany). The samples had microhardness of 16-18 GPa, and shrinkage, in relation to initial pellet, was 21-22%.

The radiographic investigation of phase structure of this ceramics (Al_2O_3 (200 nm) - 95%, MgO (73 nm) - 2%, Al_2O_3 (13 nm) - 3%) showed that it consists of two phases: the main phase is $\alpha\text{-Al}_2\text{O}_3$ (46-1212), and as admixture (not more than 1 percent) there is the second phase - cubic phase MgAl_2O_4 (10-62) (spinel) with a cell parameter $a=8.077\text{ \AA}$. SEM image of such ceramics sample is presented in Fig. 4. It is shown that this ceramics is really dense, its grain size don't exceed 3-5 μm . The formation (even in small quantity) of spinel promotes to high strength and hardness of ceramics.



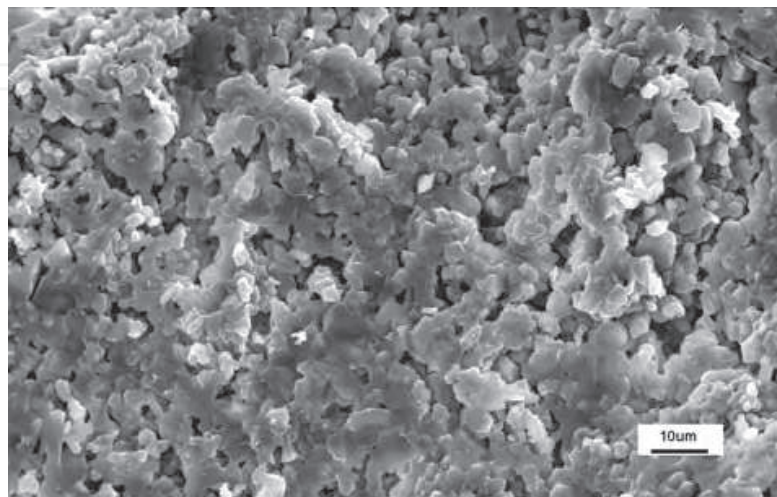
(a)



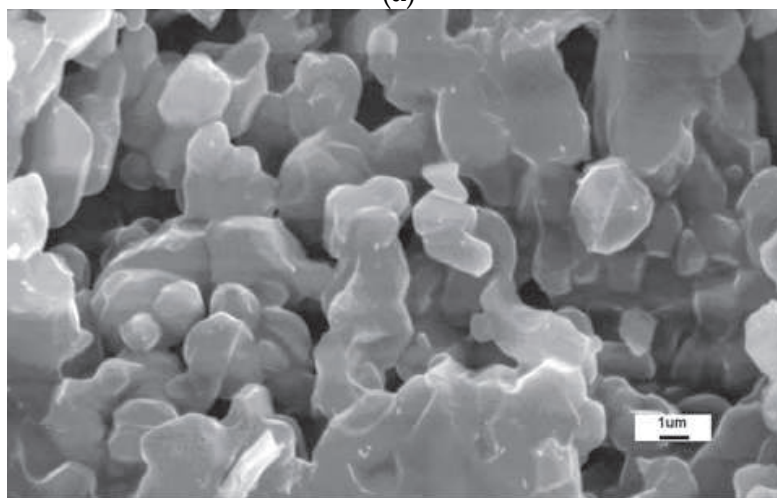
(b)

Fig. 4. SEM image of ceramics sample prepared from such components: Al_2O_3 (200 nm, 95%), MgO (73 nm, 2%), Al_2O_3 (13 nm, 3%) (a, b - different scale).

The phase structure of ceramics samples obtained from the mixture of powders, Al_2O_3 (200 nm) – 95%, MgO (73 nm) – 2%, SiO_2 (7 nm) – 3%, was analogous: the main phase is $\alpha\text{-Al}_2\text{O}_3$ (46-1212), and as admixture there is the second phase – spinel MgAl_2O_4 (10-62). SEM image of such ceramics sample is presented in Fig. 5. It is shown that this ceramics is more porous and less dense, than in Fig. 4, and less hard.



(a)



(b)

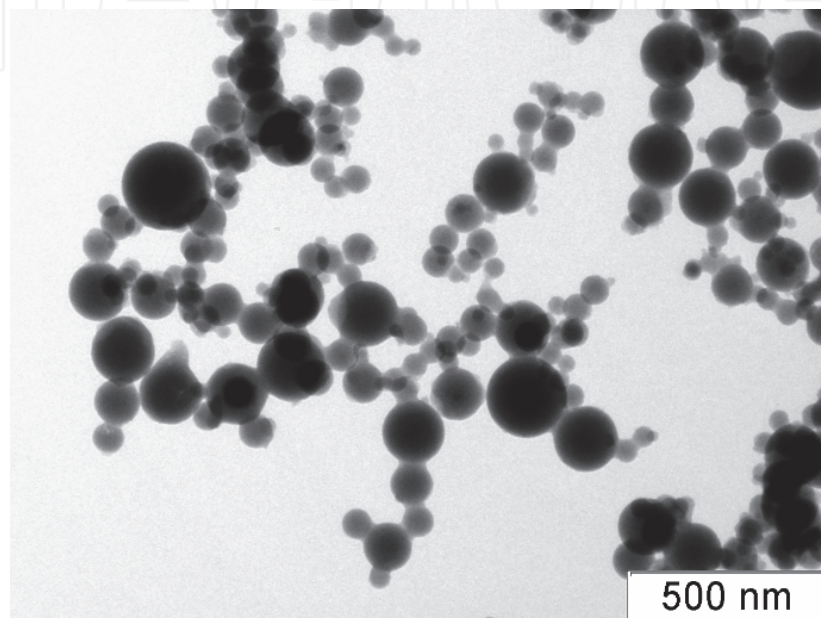
Fig. 5. SEM image of ceramics sample prepared from such components: Al_2O_3 (200 nm, 95%), MgO (73 nm, 2%), SiO_2 (7 nm, 3%) (a, b – different scale).

The powders on basis of 4 μm particles powder (AM-21) had more worse (in comparison with 200 nm powder) characteristics – the continuous samples have not been obtained even at temperature $T_{max}=1500^\circ\text{C}$. The important detail is that in composition AKP-50 – SG – Aluminum Oxide C – A-380 (0.05 %) the amorphous phase was showed. The similar effect took place at replacement of A-380 powder by T-20 powder. Thus samples in respect of strength, density and microhardness remained close to samples without SiO_2 . Such property can be useful in some cases, for example, at metallization of electrotechnical ceramics.

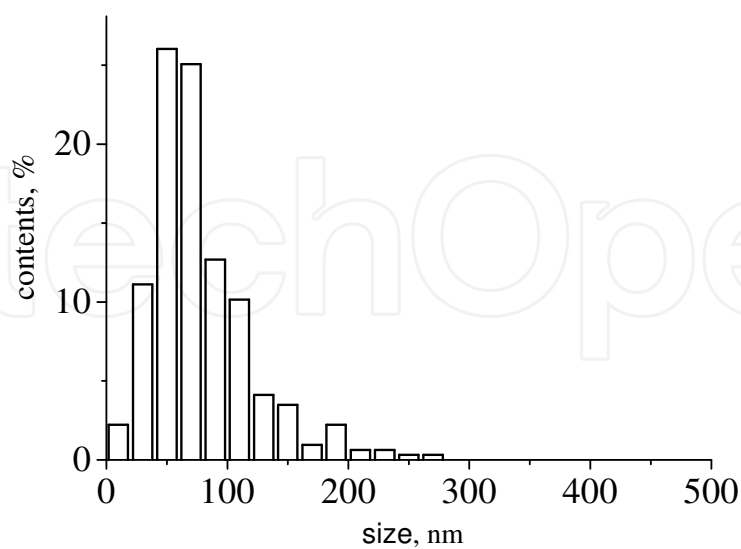
Besides from plasmachemistry powder ($d\sim 300$ nm, the Siberian chemical plant) the compact porous tablets of different open porosity, which depends on temperature of sintering, have been obtained.

3.3 Titanium dioxide TiO_2

As is well known, titanium dioxide is widely used as a basis for obtaining ceramics, while it may have photocatalytic properties. In this part of research the task was put to investigate the sintering ability of TiO_2 nanopowder obtained by the method (Lukashov et al., 1996), (Bardakhanov et al., 2008). On the data of X-ray analysis, the titania powder consisted of mainly the metastable X-ray-amorphous phase, probably, this is the fine-grained brookite (29-1360). Fig. 6 presents transmission electron microscopy image of TiO_2 nanopowder and its particle size distribution. The powder has the average size of primary particles of 78 nm.



(a)



(b)

Fig. 6. TEM image of TiO_2 nanopowder (a) and its particle size distribution (b).

The powder first was pressed, then the pressed samples sintered at temperatures of 1100°, 1200°, 1300°, 1500° and 1600°C. The higher temperature was, the higher samples strength became.

At $T_{\max} > 1300^\circ\text{C}$ the sufficiently strong (microhardness value was about 9 GPa) samples, but with big shrinkage (about 40%), have been obtained. At the same time they were of the bright yellow colour. Powders of titania, prepared at the electron beam accelerator, had high reaction activity.

3.4 Aluminium nitride AlN

As is well known, aluminium nitride possess semi-conductor properties and has been widely used in microelectronics in the form of sprayed films; ceramics from it has high thermal conductivity.

In the present work AlN obtained on the method (Lukashov et al., 1996), (Bardakhanov et al., 2008) was used for ceramics preparation. X-Ray study has shown the next phase structure of AlN powder: the phase of hexagonal AlN (25-1133) (60-70% approximately) and the phase of metal aluminium Al (4-787). The specific surface of this powder is 7 m²/g, that corresponds to the average particles size of about 250 nm. SEM image of this AlN nanopowder is presented in Fig. 7. It is shown that the powder consists of different fine-grained formations, including ones with the sizes greatly less than 250 nm.

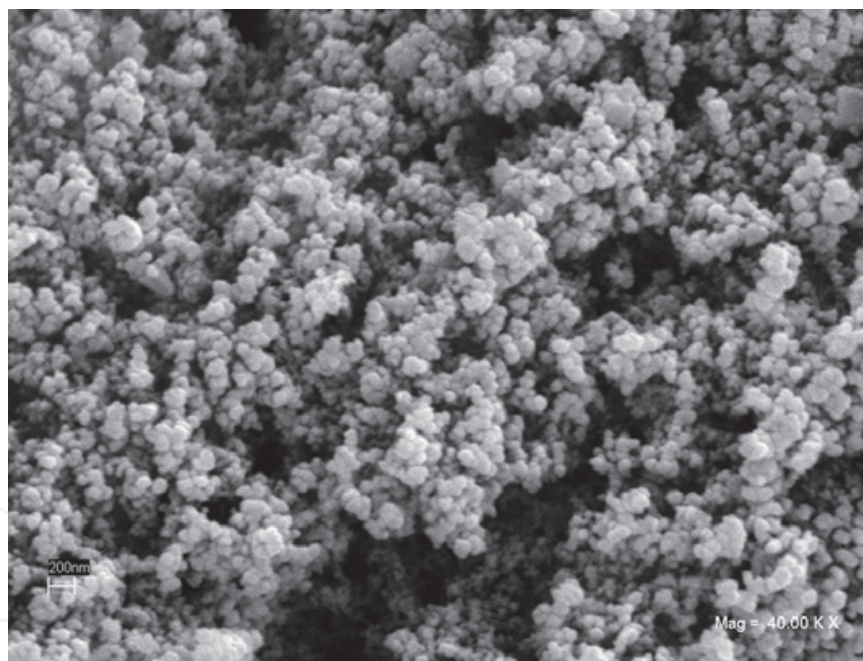


Fig. 7. SEM image of AlN nanopowder obtained with using electron accelerator (scale 200 nm on the left below).

The results of these experiments were found the next. At pressed-samples sintering of aluminum nitride in an atmosphere of air at $T_{\max} = 1600^\circ\text{C}$ the sample was almost completely oxidized to $\alpha\text{-Al}_2\text{O}_3$. At sintering in the induction furnace in an atmosphere of air-CO-CO₂ at temperature $\sim 1300^\circ\text{C}$ the sample surface for a large depth was oxidized to $\alpha\text{-Al}_2\text{O}_3$, but within the sample the powder partially sintered to the cubic phase (34-679). With sintering in the vacuum furnace at $T_{\max} \approx 1800^\circ\text{C}$ the dense nonporous strong sample with crystal structure of aluminium nitride had been produced.

X-Ray study has shown, that this sample contains the phases: main phase AlN (34-679) (with cubic structure, more than 70 wt. %), the phase of hexagonal AlN (25-1133) and traces of the α -Al₂O₃ (corundum). Hence, at sintering of nanosize powder of aluminium nitride, the change of phase structure in comparison with the initial powder (transition from hexagonal structures to cubic) has occurred, thus shrinkage of the sample was less than 20%.

3.5 Tungsten carbide WC

Ceramics based on tungsten carbide is widely used in the industry of hardmetal tools. At the same time, in some problems of atomic physics there is a need for targets on the basis of hardmetal carbides of heavy elements which have fine-grained and, at the same time, porous structure.

In these studies the WC powder (TaeguTec, South Korea) with the average particles size of 0.8 μ m (800 nm) was exploited. As the source of cobalt, the coarse grain industrial WC8 powder of WC-and-Co alloy was used. The samples, structure of which contains large quantity of WC8, had the greatest strength and density. Their porosity was practically absent. At the same time the samples obtained from mixtures with low WC8 content, and also with latex, possessed a little smaller strength, but had the essential open porosity.

3.6 - 3.7 Gadolinium oxide Gd₂O₃ and yttrium oxide Y₂O₃

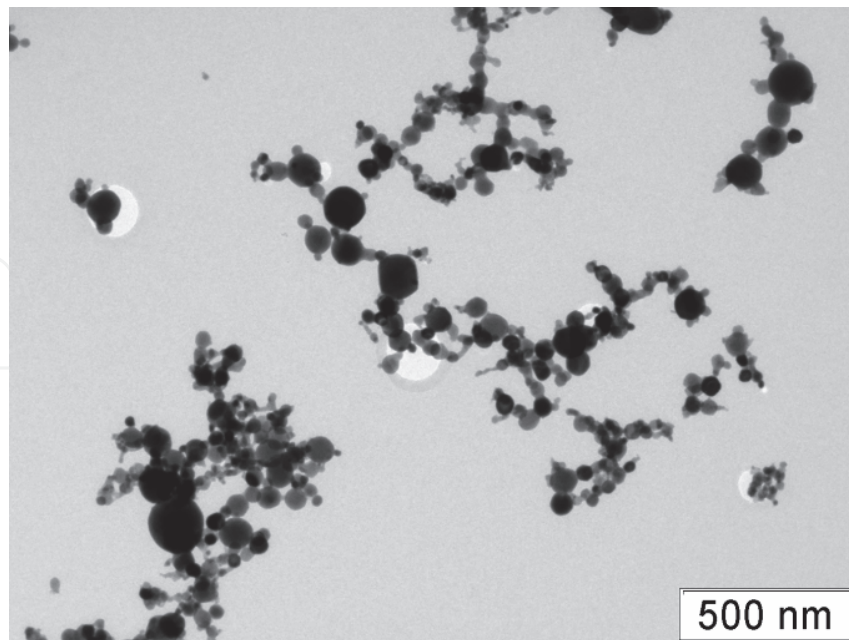
The particular interest is to obtain the ceramics from nanopowders of oxides of rare-earth elements, in particular, gadolinium and yttrium. Areas of application of materials on the basis of these substances widen constantly, at that in directions determined the technological progress (alloys of unique properties, nuclear energy, electronics, etc.).

Nanopowders of gadolinium oxide (Gd₂O₃) and yttria oxide (Y₂O₃) produced through technology of raw material evaporation by electron beam (Lukashov et al., 1996), (Bardakhanov et al., 2008) were used for preparation of submicrograin (of several micrometers) dense ceramics. These powders of gadolinium oxide and yttria oxide have the average size of primary particles of 54 nm and 32 nm and chemical purity of 99 percent.

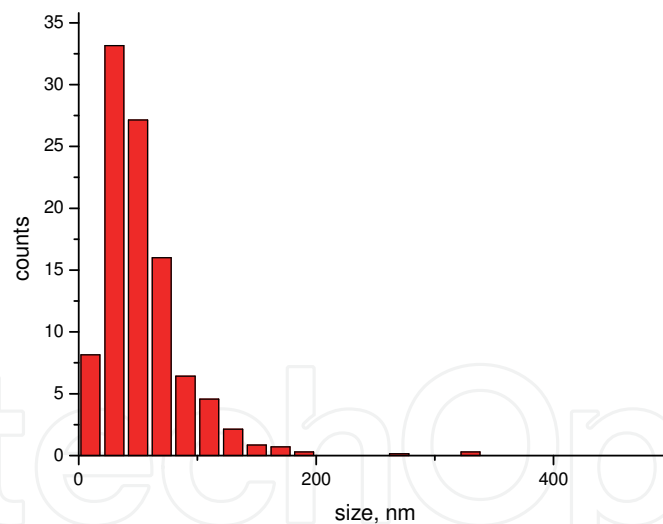
The powders of gadolinium oxide and yttrium oxide were processed in the form of monocompositions. The ceramic samples from them were obtained in a steel press mould by the method of dry pressing (without use of any binding agent and additives) at several loading-unloading cycles (at the maximum pressure 40 MPa) with subsequent sintering in the same sequence of temperature routines, thus T_{max} was 1500°C.

Radiographic research has shown that Gd₂O₃ powder enclosed monocline phase of Gd₂O₃ (JCPDS card number 42-1465), and ceramics from it enclosed (more than 75 %) cubic phase of Gd₂O₃ (43-1014). The powder of Y₂O₃ represented the mix of two phases - monocline phase of β -Y₂O₃ (47-1274) (the basic phase) and monocline phase of Y₂O₃ (44-399), and the ceramics from this powder contained only cubic phase of Y₂O₃ (43-1036).

In Fig. 8(a) there are presented the results of transmission electronic microscopy of the powder of gadolinium oxide which show that powder particles are basically united to agglomerates of chains type. As a whole it is visible that the given powder is nanosize one, that is confirmed by its particle size distribution [Fig. 8(b)]. It is visible that the main part of particles has the size less than 200 nm. The average size of primary particles is 54 nm. It is necessary to notice that many particles have facets though as a whole their form is close to sphere.



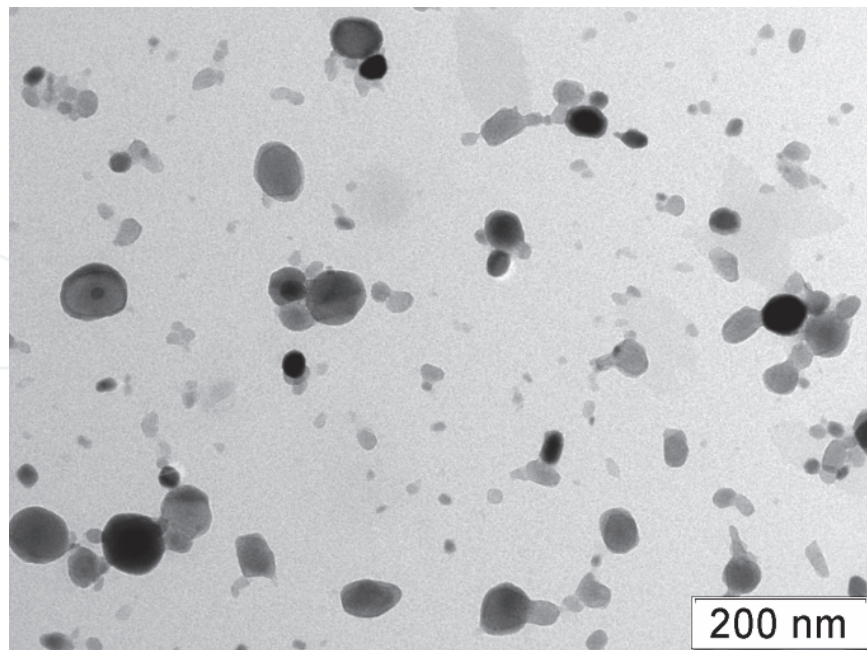
(a)



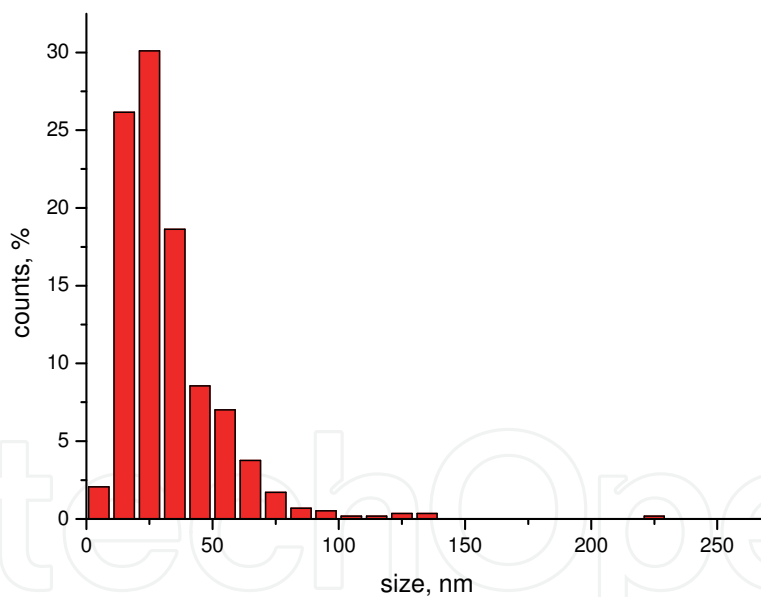
(b)

Fig. 8. TEM image of Gd₂O₃ nanopowder (a) and its particle size distribution (b).

The similar data are presented in Fig. 9 for the powder of yttrium oxide. It is visible that, in comparison with gadolinium oxide, in the powder of yttrium oxide an agglomeration is expressed more poorly, and the form of particles of yttrium oxide also is close to the spherical. The given powder also is nanosize one that is confirmed by the particle size distribution [Fig. 9(b)]. The main part of particles has the size less than 100 nm. Their average size is 32 nm.



(a)



(b)

Fig. 9. TEM image of Y₂O₃ nanopowder (a) and its particle size distribution (b).

In Fig. 10 the structure of ceramics samples of Gd₂O₃ and Y₂O₃ is shown. This figure displays the scanning electron microscope images of chip of ceramics samples prepared from Gd₂O₃ [Fig. 10(a)] and Y₂O₃ [Fig. 10(b)] nanopowders. From comparison of these figures it follows that grains of ceramics of gadolinium oxide are more isolated from each other, than grains of ceramics of yttrium oxide, and the last are good enough sintered among themselves. The size of grains of gadolinium oxide is more, and the forms of grains

of ceramics from gadolinium oxide and yttrium oxide differ. The estimation on survey photos of electronic microscopy of samples has allowed to ascertain that the maximum size of grains of gadolinium oxide is 20–25 μm , and for yttrium oxide – 10–15 μm .

As measurements of microhardness of the obtained samples have shown, for ceramics of gadolinium oxide it was approximately 6–7 GPa, and for ceramics of yttrium oxide – about 11 GPa.

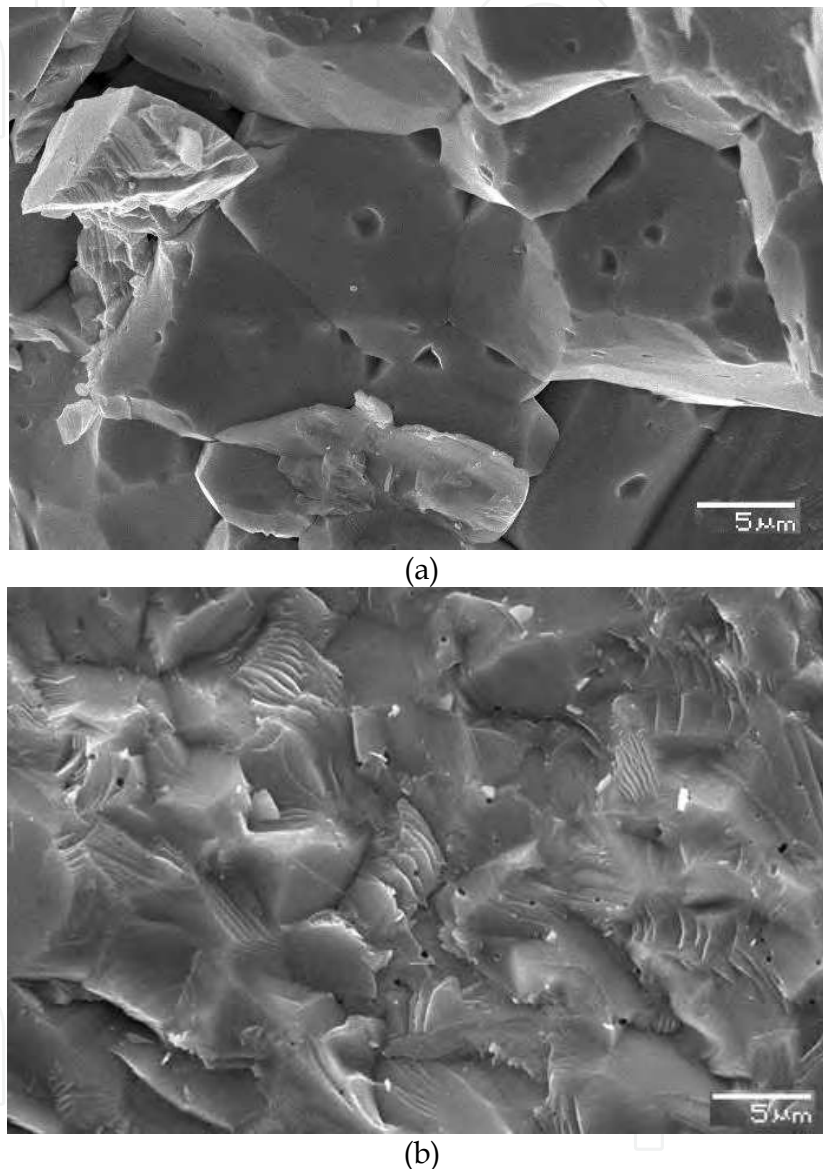


Fig. 10. SEM images of ceramics samples prepared from Gd₂O₃ nanopowder (a) and Y₂O₃ nanopowder (b).

Ultimate compression strength for ceramics of Gd₂O₃ equaled approximately 0.3 GPa, for ceramics of Y₂O₃ – about 0.4 GPa (it is possible to assume that, besides other reasons, it is explained by difference in ceramics structures).

The study of the data on fluorescence of ceramics from nanopowders of gadolinium oxide and yttrium oxide has shown the following. If radiation of the eximer KrF laser with wave length of 248 nm excites in ceramics of Gd₂O₃ the very weak reddish luminescence which

intensity is insufficient for fixing of a spectrum of fluorescence, then ceramics from Y_2O_3 is shone much more intensively. For ceramics of Y_2O_3 the radiation of wave length of 248 nm in the ultra-violet range excites phosphor in the spectrum visible range with maximum of fluorescence at about 460 nm.

It was shown that the ceramics of yttria irradiate visible light being excited by ultraviolet lasers.

4. Conclusions

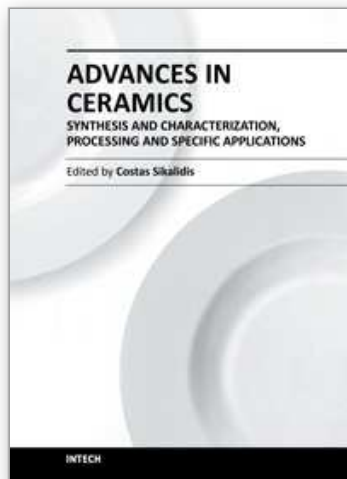
Thus, the possibility of ceramics preparation from nanopowders (including powders obtained by authors in their electron accelerator) was investigated. It was confirmed that the sintering process and the resulting ceramics depend on size and shape of particles of the powders used. The sintering temperatures of nanopowders (for example, tarkosil with an amorphous structure) are lower than those of crystalline quartz powders. The ceramic material with the fine-grained structure (with grain sizes of the order of 10–20 μm) was synthesized. The data about the shape-formation and sintering of ceramic samples of different powders combination were obtained. The dense strong samples with the microhardness of 16-18 GPa and size of several micrometers had been produced.

5. Acknowledgements

This study was partly financially supported by Grant RO RNP.2.1.2.3370.

6. References

- Bardakhanov, S.P.; Volodin, V.V.; Efremov, M.D.; Cherepkov, V.V.; Fadeev, S.N.; Korchagin, A.I.; Marin, D.V.; Golkovskiy, M.G.; Tanashev, Yu.Yu.; Lysenko, V.I.; Nomoev, A.V.; Buyantuev, M.D. & Sangaa, D. (2008). *Japan. J. Appl. Phys.*, Vol.47, p.7019.
- Bode, R.; Ferch, H. & Fratzscher, H. (2006). *Degussa Tech. Bull*, No.11, p.70.
- Colvin, V. L.; Schlamp, M.C. & Alivasatos, A.P. (1994). *Nature*, Vol.370, p.354.
- Efremov, M.D.; Volodin, V.A.; Marin, D.V.; Arzhannikova, S.A.; Goryainov, S.V.; Korchagin, A.I.; Cherepkov, V.V.; Lavrukhin, A.V.; Fadeev, S.N.; Salimov, R.A. & Bardakhanov, S.P. (2004). *JETP Lett.*, Vol.80, p.544.
- Iler, R. (1979). *Chemistry of Silica*, Wiley, New York, Vol.2.
- Korchagin, A.I.; Kuksanov, N.K.; Lavrukhin, A.V.; Fadeev, S.N.; Salimov, R.A.; Bardakhanov, S.P.; Goncharov, V.B.; Suknev, A.P.; Paukshtis, E.A.; Larina, T.V.; Zaikovskii, V.I.; Bogdanov, S.V. & Bal'zhinimaev, B.S. (2005). *Vacuum*, Vol.77, p.485.
- Lukashov, V.P.; Bardakhanov, S.P.; Salimov, R.A.; Korchagin, A.I.; Fadeev, S.N. & Lavrukhin, A.V. (1996). *Russia Patent*, 2067077.
- Zhou Xinzhang, Hulbert, D.M.; Kuntz, J.D.; Sadangi, R.K.; Shukla, V.; Kear, B.H.; Mukherjee, A.K. (2005). *Mater. Sci. Eng. A*, Vol.39, p.353.



**Advances in Ceramics - Synthesis and Characterization,
Processing and Specific Applications**

Edited by Prof. Costas Sikalidis

ISBN 978-953-307-505-1

Hard cover, 520 pages

Publisher InTech

Published online 09, August, 2011

Published in print edition August, 2011

The current book contains twenty-two chapters and is divided into three sections. Section I consists of nine chapters which discuss synthesis through innovative as well as modified conventional techniques of certain advanced ceramics (e.g. target materials, high strength porous ceramics, optical and thermo-luminescent ceramics, ceramic powders and fibers) and their characterization using a combination of well known and advanced techniques. Section II is also composed of nine chapters, which are dealing with the aqueous processing of nitride ceramics, the shape and size optimization of ceramic components through design methodologies and manufacturing technologies, the sinterability and properties of ZnNb oxide ceramics, the grinding optimization, the redox behaviour of ceria based and related materials, the alloy reinforcement by ceramic particles addition, the sintering study through dihedral surface angle using AFM and the surface modification and properties induced by a laser beam in pressings of ceramic powders. Section III includes four chapters which are dealing with the deposition of ceramic powders for oxide fuel cells preparation, the perovskite type ceramics for solid fuel cells, the ceramics for laser applications and fabrication and the characterization and modeling of protonic ceramics.

How to reference

In order to correctly reference this scholarly work, feel free to copy and paste the following:

Sergey Bardakhanov, Vladimir Lysenko, Andrey Nomoev and Dmitriy Trufanov (2011). Ceramic Preparation of Nanopowders and Experimental Investigation of Its Properties, *Advances in Ceramics - Synthesis and Characterization, Processing and Specific Applications*, Prof. Costas Sikalidis (Ed.), ISBN: 978-953-307-505-1, InTech, Available from: <http://www.intechopen.com/books/advances-in-ceramics-synthesis-and-characterization-processing-and-specific-applications/ceramic-preparation-of-nanopowders-and-experimental-investigation-of-its-properties>

INTECH
open science | open minds

InTech Europe

University Campus STeP Ri
Slavka Krautzeka 83/A
51000 Rijeka, Croatia
Phone: +385 (51) 770 447
Fax: +385 (51) 686 166

InTech China

Unit 405, Office Block, Hotel Equatorial Shanghai
No.65, Yan An Road (West), Shanghai, 200040, China
中国上海市延安西路65号上海国际贵都大饭店办公楼405单元
Phone: +86-21-62489820
Fax: +86-21-62489821

www.intechopen.com

IntechOpen

IntechOpen

© 2011 The Author(s). Licensee IntechOpen. This chapter is distributed under the terms of the [Creative Commons Attribution-NonCommercial-ShareAlike-3.0 License](#), which permits use, distribution and reproduction for non-commercial purposes, provided the original is properly cited and derivative works building on this content are distributed under the same license.

IntechOpen

IntechOpen